University of Groningen
Faculty of Mathematics and Natural Sciences
Van Swinderen Institute

Bachelor Project

Optimization of a $LiNBO_3$ Electro-Optic Field Sensor

Harmjan de Vries

Student number:S2349604

Supervised by:
Klaus Jungmann & Lorenz Willmann

July 13, 2016

Contents

1 Introduction to the field

The origin of fundamental symmetry violations such as parity and time reversal is one of the unanswered questions in the Standard Model of particle physics [3]. Precision tests of these symmetries allow for precise testing of the Standard Model. The violation of both parity and time reversal symmetry could be measured for example through the observation of permanent electric dipole moments (EDMs). If there is conserved CPT symmetry, permanent electric dipole moments also violate singular charge-parity symmetry (CP symmetry)[1]. While the EDMs that are predicted by the Standard Model are far too small to be observed in the foreseeable future, increasing the precision of experiments can rule out several specalutive models beyond the Standard Model. The ever increasing precision in EDM measurements has decreased the upper limit on EDMs and the progress that has been made is displayed in figure 1.

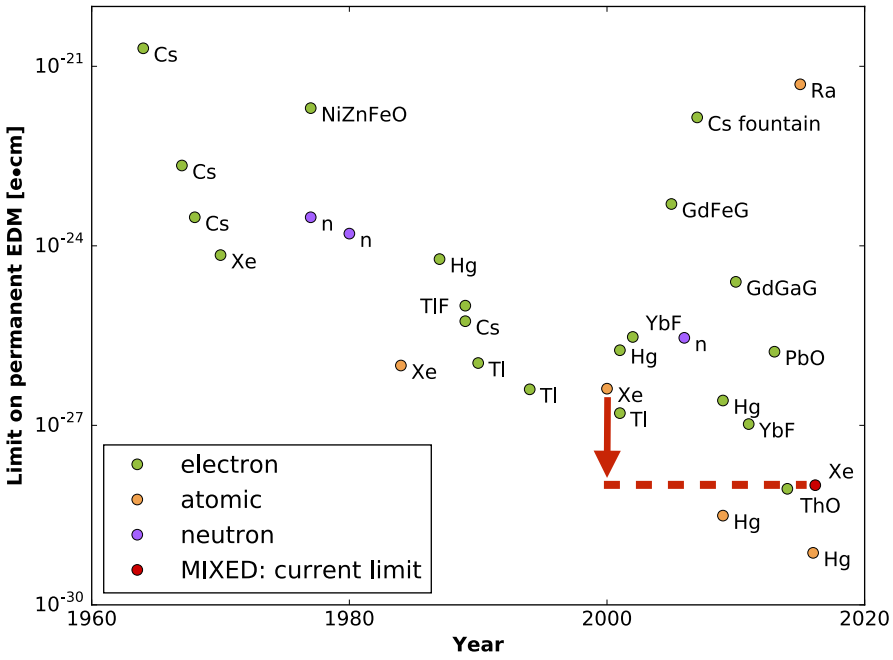

Figure 1: EDM searches that have been performed in the past decades have decreased the limit on the electric dipole moment. The red arrow indicates the recent improvement by a test experiment in Juelich on ^{129}Xe. [3]

The statistical limit δd on a permanent electric dipole moment measurement is

$$\delta d = \frac{\hbar}{E\epsilon P\eta\sqrt{\tau T N}}. \tag{1}$$

Here E is the applied external electric field, ϵ all efficiencies for detection in the experiment, η is called the enhancement factor for an EDM on the electron, T is the total measurement time, τ is the coherence time, N is the number of particles used and P is the polarization of the particles. The general statistical figure of merit for experimental searches of an EDM is

$$M = E\epsilon P\eta\sqrt{\tau T N}. \tag{2}$$

In a collaboration between the universities of Mainz, Heidelberg and Groningen and the Research Center (FZ) Juelich a search for a permanent electric dipolemoment in ^{129}Xe is performed. The experimental setup for this research is depicted in figure 2. In a magnetically shielded room, a central glass cell contains a gas sample consisting of ^{129}Xe, ^{3}He as a co-magnetometer and SF_6 as a buffer gas. A SQUID detector system continuously monitors the spin precession of both the polarized gasses in a plane perpendicular to the magnetic field.

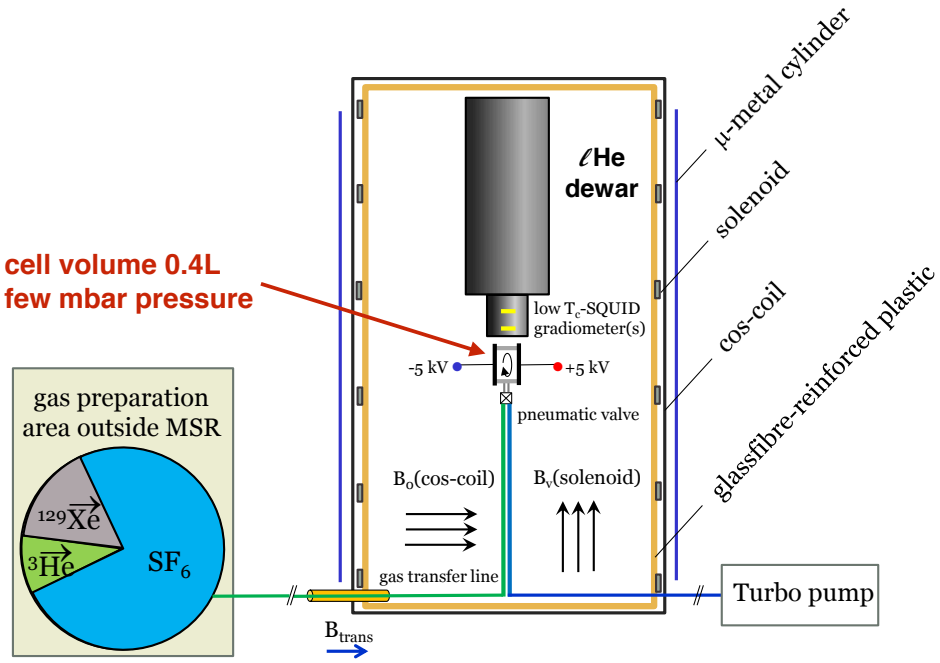

Figure 2: The experimental setup to measure an EDM in ^{129}Xe

For this measurement monitoring of the static electric field is required. Because of the extreme sensitivity of the measurement to magnetic fields, a sensor is

required that does not have any residual magnetism or magnetic field inside the shielded room. For this purpose we have developed a field sensor that exploits the optical properties of a Lithium Niobate to measure a DC electric field. The properties of Lithium Niobate make it possible to determine an electric field over a longer time, i.e 1000 seconds. In this thesis the research and optimization of a Lithium Niobate electro-optic field sensor is described. The influence of relevant parameters on the sensor signal is tested and a sensor is developed that can measure static electric fields for timescales of order of magnitudes up to a few 10^3 seconds.

2 Physics of polarization and crystal optics

2.1 Polarization of light

The polarization of light is a vector that describes the wave properties of a light beam or a photon. It is determined by the time dependent propagation of the electric-field vector. For a beam that travels in one direction, it's electric field vector will be orthogonal to the propagation direction. Defining the propagation direction as the $\hat{\mathbf{z}}$ direction, different polarizations in the **xy** plane can be distinguished.
-**Linear polarization**. The electric-field vector does not change direction as the wave propagates. The polarization is time-independent vector in the xy-plane.
-**Circular polarization**. The electric field strength is constant, but its direction rotates around the z-axis. Circular polarization is composed of two orthogonal linear polarizations with a relative phase shift of 90° and identical magnitude. Since there are two possible rotation directions around the z-axis, a distinction can be made between right-handed and left-handed polarized light.
-**Elliptical polarization**. The electric field vector rotates around the z-axis in a non-circular pattern - it describes an ellipse in the xy-plane. The field strength isn't constant for elliptical polarization, but depends on the phase. An elliptically polarized beam is composed of two linear polarized polarization with a relative angle of 90° and different magnitude.
An efficient tool to describe the polarization of light mathematically is the Jones calculus. In the next section, an overview of the Jones calculus used in this thesis is provided. The provided information on this is taken from Hecht [7] and Bahaa E. A. Saleh&Malvin Carl Teich [5].

2.1.1 Jones calculus

Jones calculus provides for describing polarized light and its interaction with optical elements. Polarization is described as a vector, the Jones Vector. Optical elements are expressed as matrices that act on Jones Vectors. Jones calculus is only applicable for polarized light.

When the propagation direction of the polarized light is defined as the $\hat{\mathbf{z}}$ direction, the electric field is

$$\mathbf{E} = \begin{bmatrix} E_{0x}e^{i(kz-\omega t+\phi_x)} \\ E_{0y}e^{i(kz-\omega t+\phi_y)} \\ 0 \end{bmatrix} = \begin{bmatrix} E_{0x}e^{i\phi_x)} \\ E_{0y}e^{i\phi_y)} \\ 0 \end{bmatrix} e^{i(kz-\omega t)}. \tag{3}$$

The Jones Vector is defined as

$$\mathbf{J} = \begin{bmatrix} E_{0x}e^{i\phi_x)} \\ E_{0y}e^{i\phi_y)} \end{bmatrix}. \tag{4}$$

It holds information about the direction, magnitude and time dependence of the polarization. The electric field of a wave with frequency ν traveling in the z direction is completely described by the Jones Vector. It is usually normalized to 1 at the starting point of a calculation. The intensity of the light is proportional to the magnitude of the Jones vector. For linear polarized light, the normalized Jones Vector takes the form

$$\mathbf{J_{linear}} = \begin{bmatrix} \cos(\theta) \\ \sin(\theta) \end{bmatrix}. \tag{5}$$

Where θ is the angle between the field of the linearly polarized light and the x-axis. Left-handed and right-handed polarization respectively have Jones Vectors

$$\mathbf{R} = \frac{1}{\sqrt{2}} \begin{bmatrix} 1 \\ j \end{bmatrix}, \quad \mathbf{L} = \frac{1}{\sqrt{2}} \begin{bmatrix} 1 \\ j \end{bmatrix}. \tag{6}$$

Elliptically polarized light is then described as a combination of linear and circular polarized light[5].

2.1.2 Polarization devices

Optical devices can alter the polarization of a light beam. In the Jones calculus, they are expressed as matrices that act on the Jones vectors. The optical devices relevant this experiment are the **linear polarizer** and the **wave retarder**.

A **Linear polarizer** is a device that only transmits linear polarized light in a certain direction, and blocks the light that is polarized in the perpendicular direction. The Jones Matrix for a linear polarizer that transmits x-polarized light is

$$\mathbf{T_{polarizer}} = \begin{bmatrix} 1 & 0 \\ 0 & 0 \end{bmatrix}. \tag{7}$$

If this matrix acts on a beam with arbitrary Jones vector (A_x, A_y), it changes the beam into a $(A_x, 0)$ linear polarized beam. It is important to note that the intensity of the wave is modulated by the polarizer, because some of the light has been blocked. The transmitted intensity of an incoming wave with Jones vector (A_x, A_y) and intensity I_0 is

$$I = I_0|A_x|^2. \tag{8}$$

A **wave retarder** retards one component of the polarization with regards to its orthogonal component. The phase of this component is delayed by Γ, the retardation constant. A wave retarder can be described by the matrix

$$\mathbf{T_{retarder}} = \begin{bmatrix} 1 & 0 \\ 0 & e^{-j\Gamma} \end{bmatrix}. \tag{9}$$

Wave retarders can be used to change any polarization into any other polarization, depending on the retardation constant. As it only changes the direction of the polarization, it leaves the intensity of the beam intact for any input polarization.
A special kind of wave retarder is the **quarter-wave retarder**.
A quarter-wave retarder is a wave retarder with $\Gamma = \pi/2$. It has the special property that it converts a linear polarized beam with Jones vector $\begin{bmatrix} 1 \\ 1 \end{bmatrix}$ into a left circular polarized beam $\begin{bmatrix} 1 \\ -j \end{bmatrix}$, and transforms right circular polarized light into linear polarized light. This property of the quarter-wave plate is useful for the creation of circular polarized light.
A circular polarizer can be made combining a quarter-wave plate and a linear polarizer. When a beam of arbitrary polarization passes through the linear polarizer and the quarter-wave plate at a relative 45° angle, the output is a circular polarized beam, assuming the incident polarization is not fully blocked by the linear polarizer. This polarization scheme is used in the experiment to create circular polarized light.

2.2 Crystal optics

The crystal in the experiment can be described as a polarization device in the Jones calculus. This crystal is $LiNbO_3$ (Lithium Niobate), which is an **Anisotropic crystal**. The optical properties of an anisotropic crystal depend on direction. To describe the optical properties of the crystal we need to analyze its refractive indices, which are calculated from the permeability tensor. Information on the refractive indices and electro-optic in the following section is based on information from M.Bordovski [4] and Bahaa E. A. Saleh & Malvin Carl Teich [5].

2.2.1 Permeability and refractive indices

The optical properties of a medium are described by it's refractive index n_i. For many media, such as water and air, the refractive index does not depend on the direction of the light. For crystals, this is often not the case. Materials for which the index of refraction depends on direction are called **birefringent**. The optical properties of a birefringent material can be described using the **Electric permittivity tensor** ϵ_{ij}. This 3-dimensional tensor describes the field permittivity of the crystal in all directions. It is symmetric, so it is characterized by up to 6 independent numbers. The elements of the permittivity tensor depend on the choice of coordinate system. The coordinate system that is most useful is the system with the **principal axes** of the crystal in the x, y and z direction. For this coordinate system, the off-diagonal elements of the permittivity tensor vanish and the only elements are the elements on the diagonal. In this coordinate system, the refractive indices are given by

$$n_x = \sqrt{\frac{\epsilon_x}{\epsilon_0}}, \qquad n_y = \sqrt{\frac{\epsilon_y}{\epsilon_0}}, \qquad n_z = \sqrt{\frac{\epsilon_z}{\epsilon_0}}. \tag{10}$$

Here ϵ_0 is the permittivity of free space.

An important mathematical trick used to determine the prinipal axes of a crystal is the **index ellipsoid** method [7].The index ellipsoid is defined

$$\sum_{ij} \eta_{ij} x_i x_j = 1. \tag{11}$$

Here η_{ij} are the elements of the impermeability tensor, defined as $\boldsymbol{\eta_{ij} = \epsilon_0 \epsilon^{-1}}$. Calculating the eigenaxes of the index ellipsoid gives the principal axes of the crystal, and the principal refractive indices are the refractive indices along those axes.
An important special case crystal is an **uniaxial** crystal. An uniaxial crystal has two equal indices of refraction. The principal refracive indices of an uniaxial crystal are denoted $n_1 = n_2 = n_o$ and $n_3 = n_e$, where n_o is called the ordinary refractive index and n_e is the extraordinary refractive index. When $n_e > n_o$,

the crystal is said to be positive uniaxial, and for $n_o > n_e$ the crystal is negative uniaxial.

2.2.2 Light propagation along a principal axis

When a light beam travels through a crystal along a principal axis, it's phase is shifted because the light travels slower in the medium. A beam that propagates along a principal axis in the z direction, and is polarized in the direction of another principal axis in the x-direction, travels with a velocity of c/n_x. In the crystal its phase is shifted by $\phi = n_x k d$, where k is the wave number and d is the distance travelled through the medium.
When a beam is polarized along both of the principal axes, the polarization of the beam changes. The phase shift in both directions is different, which causes the polarization in the direction with the highest refractive index to be retarded. The crystal acts as a **wave retarder**. The difference between the phase shifts gives the relative phase shift, which is the retardation constant as described in section 2.1.2. The retardation constant is $\Gamma = \phi_y - \phi_x = (n_x - n_y)kd$.

The goal of the experiment is measuring an electric field with an electro-optic crystal. This can be done because the refractive indices of an electro-optic crystal change when subjected to an electric field. The effects that describe this are called the **Pockels effect** and the **Kerr effect**.

2.2.3 The Pockels and Kerr effects

Both the Pockels and the Kerr effect can be described by writing the refractive index $n(E)$ as a function of the electric field E. In general, the refractive index can be written as

$$n(E) = n + aE + a_2E^2 + ... \tag{12}$$

In most materials, the terms with order 2 and higher are irrelevant. In the case of the **Pockels effect**, the a_2E^2 term is also negligible, so the refractive index is linear dependent on the electric field. For the **Kerr effect**, the aE term is negligible and the refractive index has a quadratic dependence on the electric field. The main focus of this research is the Pockels effect, since the crystal used for the experiment exhibits the Pockels effect. The equation for the Pockels effect is usually written as

$$n(E) = n - \frac{1}{2}rn^3E. \tag{13}$$

Where the coefficient r is called the Pockels coefficient. It typically has a value between 10^{-12} and 10^{-10} m/V, so changes in the refractive index due to electric fields are relatively small.
For anisotropic media, such as $LiNbO_3$, the Pockels effect can not be described by only one Pockels coefficient. As well as the refractive index, the electro-optic effects depend on direction. For these anisotropic media, we use a tensor, which describes the electro-optic effect in all directions. The tensor r_{ijk}, which is called the electro-optic tensor, acts on the impermeability tensor as

$$\eta_{ij}(\mathbf{E}) = \eta_{ij}(\mathbf{0}) + \sum_k r_{ijk}E_k. \tag{14}$$

The tensor r_{ijk} is a third-rank tensor, but because η_{ij} is symmetric and has only 6 independent elements, r_{ijk} can be expressed as a 6X3 matrix. To do this, the tensor r_{ijk} is replaced by a tensor r_{Ik}, where I goes from 1 to 6. The element I of R_{Ik} that corresponds to element ij of r_{ijk} is shown in the table below.

j	i=1	2	3
1	1	6	5
2	6	2	4
3	5	4	3

With this equation for the impermeability tensor, the new index ellipsoid can be calculated using equation 10. The index ellipsoid is changed because of the electric field, and there is a new set of principal axes.

3 $LiNbO_3$ dynamic wave retarder

The crystal used in the experiment is a $LiNbO_3$ crystal, which is an anisotropic Pockels crystal. In this experiment, it is used as a **dynamic wave retarder**. Because its indices of refraction depend on the electric field, the retardation constant along a principal axis depends on the electric field. The crystal can be used as an electric field sensor, because its effects on an incoming polarized beam depend on field strength.

3.1 $LiNbO_3$ electro-optic properties

In absence of an electric field, $LiNbO_3$ is an uniaxial crystal. Light that propagates along the extraordinary refractive axis of an uniaxial crystal propagates slower than c, but its polarization does not change. When an electric field is applied the ordinary refractive indices are changed by the Pockels effect. The crystal is no longer uniaxial and it acts as a wave retarder.
We define the ordinary refractive axes, the axes with the same refractive index, in the $\hat{\mathbf{x}}$ and $\hat{\mathbf{y}}$ direction, and the extraordinary axis in the $\hat{\mathbf{z}}$ direction. The Pockels coefficients of $LiNbO_3$ in this coordinate system take the form[2]

$$r_{ik} = \begin{pmatrix} 0 & -r_{22} & r_{13} \\ 0 & r_{22} & r_{13} \\ 0 & 0 & r_{33} \\ 0 & r_{51} & 0 \\ 0 & r_{51} & 0 \\ -r_{22} & 0 & 0 \end{pmatrix}. \tag{15}$$

Equation 12 can now be used to calculate the impermeability tensor from the Pockels coefficient

$$\eta_{ij}(\mathbf{0}) + \sum_k r_{ijk} E_k = \begin{pmatrix} \frac{1}{n_o^2} - r_{22}E_2 + r_{13}E_3 & r_{22}E_1 & r_{51}E_1 \\ r_{22}E_1 & \frac{1}{n_o^2} + r_{22}E_2 + r_{13}E_3 & r_{51}E_2 \\ r_{51}E_1 & r_{51}E_2 & \frac{1}{n_e^2} + r_{33}E_3 \end{pmatrix}. \tag{16}$$

The index ellipsoid is calculated from the impermeability tensor. x_1, x_2 and x_3 denote the x, y and z directions

$$\begin{aligned} &(\frac{1}{n_o^3} - r_{22}E_2 + r_{13}E_3)x_1^2 + (\frac{1}{n_o^2} + r_{22}E_2 + r_{13}E_3)x_2^2 \\ &+(\frac{1}{n_o^2} + r_{33}E_3)x_3^2 + 2x_2x_3r_{51}E_2 + 2x_1x_3r_{51}E_1 - 2x_1x_2r_{22}E_1 = 1. \end{aligned} \tag{17}$$

It will be shown that for light propagating in the $\hat{\mathbf{z}}$ direction the polarization output does not depend on E_3, the field parallel to the laser beam.

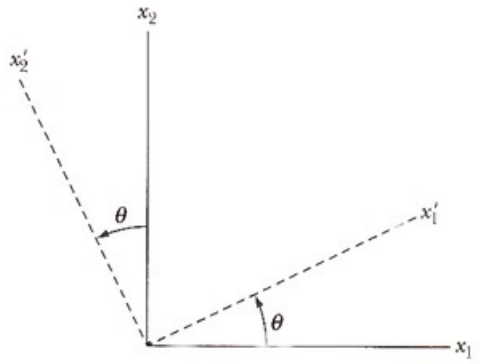

Figure 3: A rotated coordinate system is used to calculate the index ellipsoid.

When the light propagates along the $\hat{\mathbf{z}}$ direction, the index ellipsoid is simplified greatly and takes the form of a two-dimensional ellipse

$$(\frac{1}{n_o^3} - r_{22}E_2 + r_{13}E_3)x_1^3 + (\frac{1}{n_o^2} + r_{22}E_2 + r_{13}E_3)x_2^2 \\ -2x_1x_2r_{22}E_1 = 1. \tag{18}$$

To find the eigenaxes of the index ellipsoid the equation is transformed into a coordinate system rotated by θ, as shown in figure 3

$$\begin{pmatrix} x_1' \\ x_2' \end{pmatrix} = \begin{pmatrix} \cos(\theta) & \sin(\theta) \\ -\sin(\theta) & \cos(\theta) \end{pmatrix} \begin{pmatrix} x_1 \\ x_2 \end{pmatrix}. \tag{19}$$

In the new coordinate system, the index ellipsoid becomes

$$(\frac{1}{n_o^2} - r_{22}E_2 + r_{13}E_3)(x_1'^2\cos^2\theta + x_2'^2\sin^2\theta - 2x_1'x_2'\cos\theta\sin\theta) \\ +(\frac{1}{n_o^2} + r_{22}E_2 + r_{13}E_3)(x_1'^2\sin^2\theta + x_2'^2\cos^2\theta + 2x_1'x_2'\cos\theta\sin\theta) \\ -r_{22}E_2(x_1'^2\cos\theta\sin\theta + x_1'x_2'\cos^2\theta - x_1'x_2'\sin^2\theta - x_2'^2\sin\theta\cos\theta) = 1. \tag{20}$$

An ellipse is characterized by the equation $ax^2 + by^2 = 1$ with principal axes x and y. For equation 18 this means that the coordinates x_1, x_2 coincide with the eigenaxes of the ellipse when there are no cross terms. Setting the sum of the cross terms in the equation equal to zero gives us the coordinate transformation angle θ as a function of the electric field

$$4r_{22}E_2\cos\theta\sin\theta - 2r_{22}E_1(\cos^2\theta - \sin^2\theta) = 0$$

$$\frac{E_2}{E_1} = \frac{\cos^2\theta - \sin^2\theta}{\cos\theta\sin\theta} = \frac{1}{\tan(2\theta)}. \tag{21}$$

The angle ϕ between the electric field vector $\mathbf{E_{12}} = \mathbf{E_1} + \mathbf{E_2}$ can now be related to the orientation of the eigenaxes

$$\theta = \frac{\pi/2 - \phi}{2}. \tag{22}$$

The rotation of the applied electric field in the (x_1, x_2) plane causes the optical eigenaxes to rotate in the opposite direction and twice as slow. The optical eigenaxes of the ellipsoid can now be used to calculate the indices of refractive along the eigenaxes and the induced birefringence for any applied field $\mathbf{E}$. The indices of refraction are given by the $x_1'^2$ and $x_2'^2$ terms in equation 18.

$$\frac{1}{n_1^2} = \frac{1}{n_o^2} + r_{13}E_3 - r_{22}E_2\cos(2\theta) - r_{22}E_1\sin 2\theta \tag{23}$$

$$\frac{1}{n_2^2} = \frac{1}{n_o^2} + r_{13}E_3 + r_{22}E_2\cos(2\theta) + r_{22}E_1\sin 2\theta \tag{24}$$

E_1 and E_2 can be expressed in terms of the total electric field vector E_{12} in the xy-direction. When ϕ is the angle between E_{12} and the x-axis, $E_1 = E_{12}\cos(\phi)$ and $E_2 = E_{12}\sin(\phi)$. Together with equation 4.32 the θ terms vanish from the equation. With the use of differential calculus $\mathrm{d}n = -(n^3/2)d(1/n^2)$ which is justified by the fact that changes in the refractive indices due to fields are relatively small compared to n_0[6], the equation is rewritten as

$$n_1 = n_0 - \frac{n_0^3}{2}(r_{13}E_3 - r_{22}E_{12}) \tag{25}$$

$$n_2 = n_0 - \frac{n_0^3}{2}(r_{13}E_3 + r_{22}E_{12}). \tag{26}$$

The birefringence of the crystal for a beam in the z-direction is equal to the difference in refractive indices

$$\Delta n = n_2 - n_1 = n_0^3 r_{22}E_{12}. \tag{27}$$

This proves that the birefringence of the crystal for a beam in the z-direction does not depend on the E_3 component of the electric field. The birefringence also doesn't depend on the direction of the electric field in the xy-plane, only on the magnitude of the field in this plane E_{12}.
Because the birefringence of the crystal depends on electric field, the electric field can be measured by measuring the change in polarization caused by this birefringence. An incident beam with circular polarization will undergo a phase retardation in the crystal. The phase retardation is proportional to the electric field and given by the equation [4]

$$\Gamma = \frac{2\pi}{\lambda}\Delta n l = \frac{2\pi}{\lambda}n_o^3 r_{22}E_{12}l. \tag{28}$$

The retardation in the crystal causes the circular polarized light to become elliptical. An experimental setup can be made to measure the birefringence by analyzing the polarization change of circular polarized light.

3.2 Experimental setup

The setup used to measure the electric field is shown in figure 4 and 5.

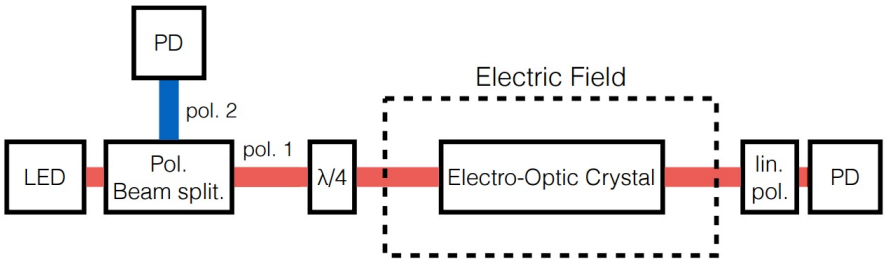

Figure 4: A schematic overview of the experimental setup used to generate and measure an electric field. The PD's in the picture indicate the photodiodes, and $\lambda/4$ indicates the position of th quarter-wave plate.

As the light from the LED leaves the fiber, it is first linear polarized by the polarizing beamsplitter, and then circular polarized by the quarter-wave plate. Apertures are used to ensure that all the light goes through the crystal. The light passes through the crystal along its extraordinary refractive axis. The crystal is placed between two electrodes that create the electric field, which can be controlled externally. The polarization of the light as it leaves the crystal is measured with a rotatable linear polarizer, also named the analyzer. Behind the analyzer is a photodiode to measure the intensity of the light as it leaves the analyzer. The second beam from the beamsplitter is captured by another photodiode, which is useful to measure the relative intensity of the light before it passes through the polarization scheme.
Both photodiodes are connected to the data acquisiton system via a voltage-to-frequency converter. The voltage-to-frequency converter changes the analog signal from the photodiodes into a count rate. The count rates range from 0 to $2.3 * 10^5$ counts. A count rate of $1.038 \pm 0.001 * 10^5$ corresponds to 0V and the maximum count rate of $2.3 * 10^5$ corresponds to a photodiode voltage of 10V. The values below $1.038 * 10^5$ indicate a negative voltage. The voltage-to-frequency converter can be set to amplify the signal 1, 10 or 100 times. For different measurements a different amplification setting is used, so the count rate does not always correspond to the same intensity in different graphs. Be-

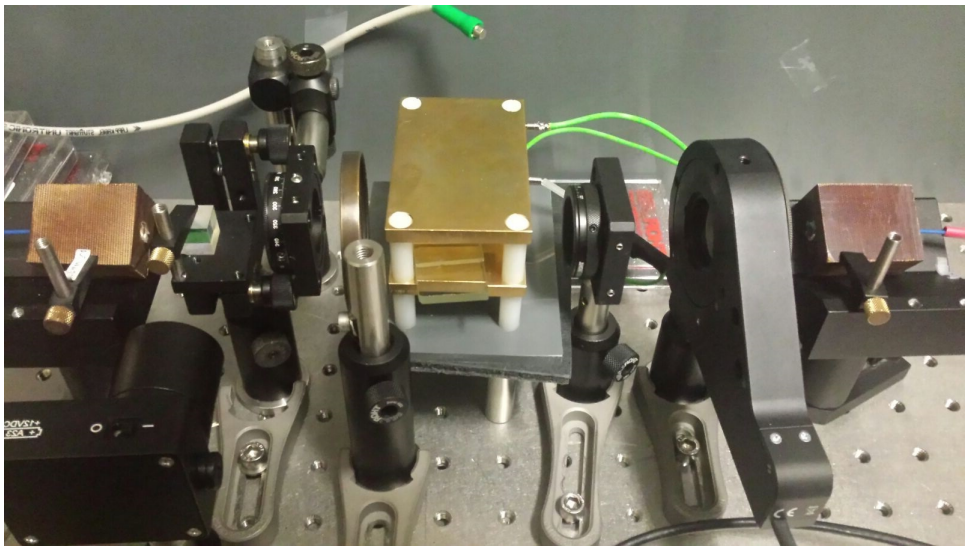

Figure 5: A photo of the experimental setup. The optical fibers are mounted in the brown blocks. The light leaves the fiber from the block on the left via a lens and enters the polarizing beamsplitter. One of the two beams from the polarizing beamsplitter is captured by the photodiode at the bottom of the photo, and the other passes through the quarter-wave plate mounted in a rotatable stage. Between the quarter-wave plate and the crystal is an aperture. Between the two gold-colored electrode plates that generate the electric field is the Lithium Niobate crystal. The light from the crystal passes through a second aperture before it reaches the analyzer, which is mounted in the large black rotatable stage on the right. As the light leaves the analyzer it is captured in the second optical fiber via a lens. This optical fiber is connected to the second photodiode.

cause only a relative intensity change due to the electric field is relevant for this experiment, measuring the intensity in counts is sufficient and the absolute luminosity in the photodiode is not derived.

In the next sections the optimization of this electric field sensor is discussed and the accuracy of the sensor for time scales of 10^2 10^4 seconds will be measured.

4 Optimizing the sensor

Several factors affect the preciseness of the sensor and for an accurate measurement we need to optimize the parameters that influence the sensor. The first requirements for a good measurement are good control of the input polarization and light intensity and an accurate way to measure the polarization as it leaves the crystal. When these requirements are met we measure the influence of the analyzer angle on the signal. The angle is searched for which the change in the signal due to an electric field is maximal. When this signal is maximized, research can be done on the effectiveness of the sensor for static fields on timescales of $10^2 - 10^4$ seconds.

4.1 Input and output polarization

4.1.1 Intensity of the beam

To optimize the alignment of the initial light beam and polarization devices, the crystal is removed from the setup. Since all elements should be examined separately, all elements except the apertures are removed for the first measurement, so the light from the LED can be measured. It can not be assumed that the LED intensity scales perfectly linear with the input power, so the intensity of the LED for different input powers is measured in the photodiode. The relative intensity as a function of LED voltage is shown in figure 6. Here the LED voltage goes from 0 to 5 volt with steps of 0.2V, and the count rate in the photodiode is shown on the y-axis. For every value of the voltage, the count rate was measured for 30 seconds.

From this figure, it can be concluded that the power dependence is not exactly linear: the intensity increases slightly slower for higher voltages. Nonetheless the linear approximation is accurate, since the highest deviation is approximately 2%.

4.1.2 Testing the linear polarizers

The efficiency of the linear polarizers can be examined by adding the polarizing beamsplitter and the analyzer to the setup. When both of the linear polarizers work as intended, there should be an angle of the rotating polarizer for which no light can reach the photodiode, because the linear polarizer directions are perpendicular. A 360° scan of the light from the initial linear polarizer is shown in figure 7.

This sinusoidal dependence on the angle is the expected result. It can be seen from the graph that there is an angle for which the count rate almost reaches the zero value, but the angular resolution is not enough to see if the zero value is reached. Adapting the analyzer angle with steps of 1° between 100 and 120° and measuring the intensity for these angles, we have measured that the count rate reaches it's minimum value of $(1.0365 \pm 0.0003 * 10^5)$ counts at an angle of 114°. This means that both of the linear polarizers work as intended, and

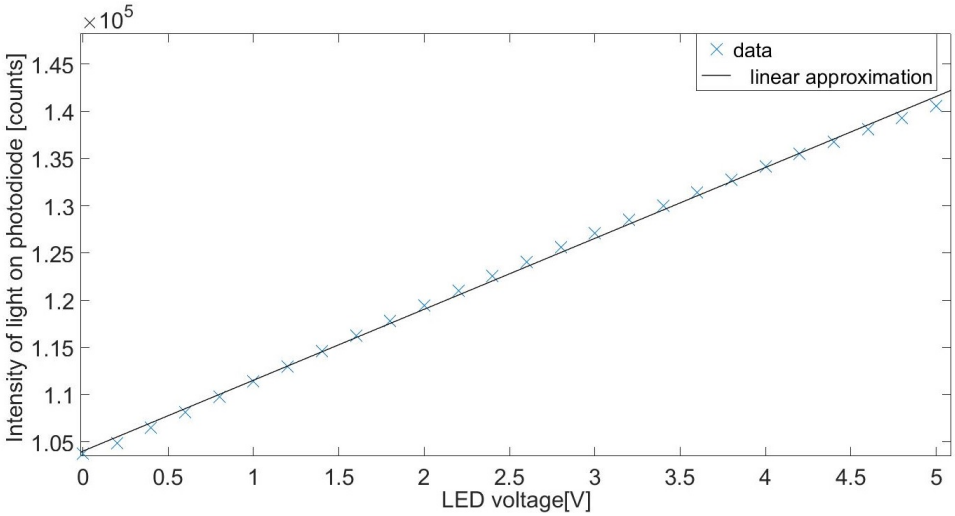

Figure 6: Intensity of the light on the photodiode as a function of the LED voltage. The uncertainty in this measurement is approximately 30-100 counts, where the error is highest for the highest voltage. No error bars have been provided because such small error bars would be invisible.

the amount of light that is transmitted by the analyzer when the polarizers are orthogonal is less than the background light. From the measured angle it can be concluded that the linear polarizer in the rotating frame has its polarization direction at a 24° angle from the polarization direction of the initial linear polarizer, because the polarizers are orthogonal at an angle of 114 °.

4.1.3 Creating circular polarization

As explained in 2.1.2, a circular polarizer can be created by combining a quarter-wave plate and a linear polarizer. When linear polarized light enters the quarter-wave plate at a 45° angle, the quarter-wave plate transforms the light into circular polarized light. Because the analyzer isn't perfectly mounted in its rotatable frame, it can't be assumed that the rotatable frame angle corresponds to the angle at which the quarter-wave plate is aligned. Fortunately, there are other ways to determine the orientation of the quarter-wave plate. For circular polarized light, rotating the analyzer does not change the signal in the photodiode, because circular polarized light is polarized equally in all directions. It is therefore possible to measure how circular the polarization is by measuring how much the count rate changes when the analyzer is rotated. Finding the quarter-wave plate angle for which the count rate changes the least when rotating the analyzer gives the angle for which the light is closest to a circular polarization. This method of circularly aligning the quarter-wave plate is used throughout

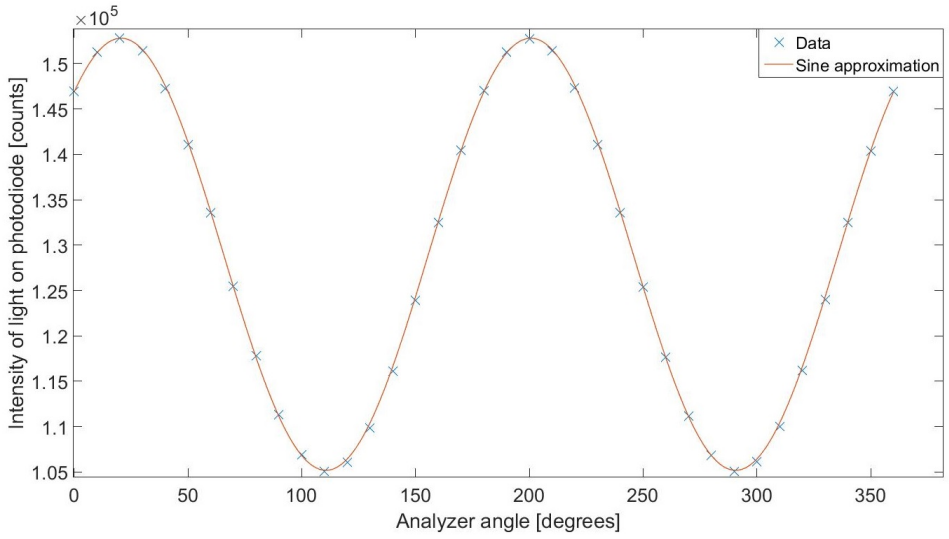

Figure 7: Intensity of the light as it leaves the initial linear polarizer, as a function of the analyzer angle.The uncertainty in the measurement is 50-100 counts for each angle. No error bars have been displayed because such small error bars would become invisible. The linear approximation of this data shows that the intensity dependence on voltage is not exactly linear.

the entire experiment.
Using this method it becomes clear that the quarter-wave plate does not operate perfectly. Even at the angle for which the intensity depends the least on the analyzer angle, the signal still changes when the analyzer is rotated. A scan of the 'circular' polarized light is shown in figure 8.

As can be seen in the figure, the light is not exactly circular polarized. There is a difference of $5.5 * 10^5$ counts between the minimum and the maximum, which corresponds to 22% of the signal. For every one of the different alignments that have been made during the experiment (see chapter 5.3), the light couldn't be made more circular than this. Though a perfectly circular polarization would result in better measurements, it is not required and the elliptical polarization is sufficient to measure the electric field with the crystal.

4.2 Aligning the crystal

Now that circular polarized light is created, the crystal is added to the setup. It is placed between the two electrodes. The crystal is aligned in such a way, that the light propagates along the extraordinary refractive axis, which is the $\hat{\mathbf{z}}$ axis. Apertures are used to make sure that the light passes through the middle of the crystal. This is done to avoid reflections in the side of the crystal and

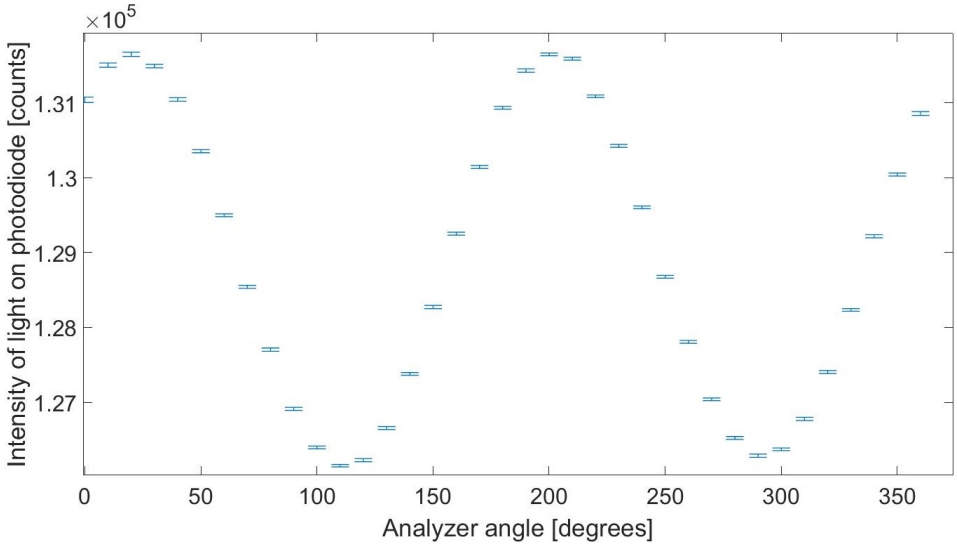

Figure 8: Intensity as a function of analyzer angle for 'circular' polarized light as it leaves the quarter-wave plate. The quarter-wave plate angle is chosen for as such that the intensity depends the least on analyzer angle. The provided error bars are the maximum and the minimum intensity for the respective analyzer angle.

light hitting the photodiode that did not pass through the crystal.

4.2.1 Preciseness of the alignment

It is important to note that though the crystal theoretically has no birefringence when light propagates along the $\hat{\mathbf{z}}$ axis, it still has a birefringence in practice. This birefringence is present because it is impossible to create a beam that is purely aligned in the direction of the extraordinary refractive axis. The divergence of the beam, impreciseness of the alignment and a non-perfect crystal cut contribute to this and cause the measured birefringence of the crystal at $E = 0$. Because these factors cause a birefringence the polarization can become more elliptical as it leaves the crystal even when no electric field is applied.
Since the setup has been built several times, the alignment of the crystal was never exactly the same. Because the output signal depends so strongly on the preciseness of the alignment, there are large differences in the shape of the output signal for the different experiments. In many cases, the setup was realigned several times in order to create an optimal signal.

4.2.2 The crystal as electric field sensor

With the crystal and the polarization devices aligned, the crystal can now be used as an electric field sensor. To optimize it's function as an electric field sensor, the two parameters that have to be optimized are the magnitude of the signal and the charge relaxation time.

-Magnitude of the signal

In order to make a precise electric field measurement, it is important that the count rate changes significantly due to the applied electric field. The count rate change that appears when an electric field is applied has to be larger than the other factors that affect the count rate. The most important of these factors are electronic noise, change in background light, LED intensity fluctuations, ground fluctuations and temperature fluctuations. The electronic noise amplitude is always smaller than 10 counts. The background light was measured by measuring the difference in counts that occurs by covering the photodiode. Background light contributes to less than 200 counts. The fluctuations that appear in the signal due to temperature changes and ground fluctuations will be discussed in chapter 5.6. These fluctuations vary wildly. Fluctuations of up to 500 counts have been measured. For a precise measurement a signal that is significantly larger than the above mentioned factors is required. The magnitude of the field-dependence of the signal can be expressed in counts/(V/cm). During the experiment, the usual magnitude of the signal for a good alignment is 5000-10000 counts/(kV/cm).

-Charge relaxation time

When the electric field is applied to the crystal over a longer time, the crystal will exhibit the **space charge effect**[4]. The crystal has finite resistivity, so the free charges in the crystal will start drifting along the electric field lines and accumulate on crystal boundaries. An electric field with orientation opposite to the original internal field is generated. This causes the sensor output to decrease over time, since the electro-optic effect depends on the internal field rather than the external field. The speed of the space charge effect depends on the density of free charge carriers, which is proportional to crystal conductivity. The decay is exponential, and is expressed as

$$E(t) = E_m e^{-\frac{t}{\tau}}. \tag{29}$$

Here the constant τ indicates how fast the internal electric field decays. It is called the *charge relaxation time constant*.

In the upcoming sections, the factors that influence the charge relaxation time and the magnitude of the signal will be measured and adapted, in order to optimize the sensor.

4.3 Optimizing the signal magnitude

In section 3.1 it has been shown that the birefringence of the crystal does not depend on the z-component of the elecric field, and is also independent of the field direction in the xy-plane. In this experiment the electric field is chosen in the y-direction in the coordinate system as defined before. While the magnitude of the birefringence doesn't depend on the field direction in the xy-plane, the orientation of the field does change the principal refractive axes in this plane. Therefore the magnitude of the signal depends on the angle of the analyzer and there is an optimal angle for which the electric field causes the highest change in the signal.
It has been shown in section 3.1 that the rotation of the principal refractive axes θ depends on the electric field angle ϕ in the xy-plane.

$$\theta = \frac{\pi/2 - \phi}{2} \tag{30}$$

In the experiment the electric field orientation is fixed in the x_2 direction. This gives $\phi = \pi/2$, so the coordinate system (x_1', x_2') is the same as the orignal coordinates x_1, x_2 because $\theta = 0$
. In order to find the optimal angle of the analyzer we first calculate the theoretical output polarization using the Jones calculus. The incoming wave with circular polarization is described by the Jones vector

$$\mathbf{L_i} = \frac{1}{\sqrt{2}} \begin{pmatrix} 1 \\ i \end{pmatrix}. \tag{31}$$

To obtain the Jones representation of the light as it leaves the crystal, the matrix for a wave retarder with retardation constant Γ is applied to the circular polarized light. The resulting polarization as the light leaves the crystal is

$$\mathbf{L_c} = \frac{1}{\sqrt{2}} \begin{pmatrix} e^{i\frac{\Gamma}{2}} & 0 \\ 0 & e^{i\frac{\Gamma}{2}} \end{pmatrix} \begin{pmatrix} 1 \\ i \end{pmatrix} = \frac{1}{\sqrt{2}} \begin{pmatrix} \cos(\Gamma/2) + i\sin(\Gamma/2) \\ i\cos(\Gamma/2) - \sin(\Gamma/2) \end{pmatrix}. \tag{32}$$

The Jones vector of the light as it leaves the analyzer after going through the crystal is a function of the analyzer angle α. The expression for the rotation of an optic element by an angle α is used from Bahaa E. A. Saleh et al. [5].

$$\mathbf{L_a} = \frac{1}{\sqrt{2}} \begin{pmatrix} \cos(\alpha) & -\sin(\alpha) \\ \sin(\alpha) & \cos(\alpha) \end{pmatrix} \begin{pmatrix} 1 & 0 \\ 0 & 0 \end{pmatrix} \begin{pmatrix} \cos(\alpha) & \sin(\alpha) \\ -\sin(\alpha) & \cos(\alpha) \end{pmatrix} \begin{pmatrix} \cos(\Gamma/2) + i\sin(\Gamma/2) \\ i\cos(\Gamma/2) + \sin(\Gamma/2) \end{pmatrix} \tag{33}$$

Now we have a set of matrix multiplications that includes all optical elements, the intensity in the photodiode can be calculated as it is the product of L_a and its complex conjugate. The approximation that $\sin(\Gamma/2) = \Gamma/2$ can be used and the expression becomes dependent on Γ as

$$I_{out} = \mathbf{L_a}\mathbf{L_a}* \propto \Gamma \sin(2\alpha). \tag{34}$$

This equation would imply that the crystal is best aligned at at $\alpha = \pi/4 + n*\pi/2$

with respect to the x-axis, since the signal depends the most on Γ for these angles.
We can test this with an oscillating electric field. A 0.5 Hz, 0.25kV/cm electric field is applied to the crystal and the intensity signal in the photodiode will to oscillate due to the oscillating applied electric field. Because the magnitude of this oscillation corresponds to the signal dependence on the electric field, we want to maximize the oscillation of the intensity.
A measurement is set up where the rotating stage is set to rotate a 10° angle every 60 seconds while the oscillating field is applied to the crystal. This measurement is stored and the data is analyzed with MATLAB and the amplitude oscillation is determined for every analyzer angle. The result of this is shown in figure 9.

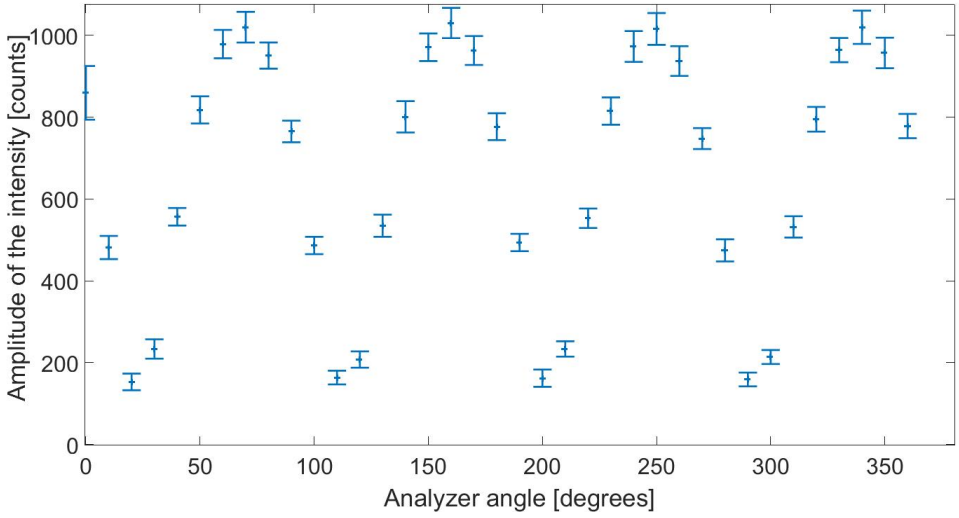

Figure 9: Amplitude of the intensity fluctuation due to a 0.5Hz electric field as a function of analyzer angle. The provided error bars are calculated from the deviation in amplitude of single oscillations measured for an angle.s

This measurement corresponds with what we expected, since there is a $|\sin(2\alpha)|$ dependence of the signal on the angle. As we know from section 4.1.2, the analyzer is shifted by 24° with respect to the x-axis in its mount. For this reason the maxima in figure 9 are also shifted by 24° with respect to the predicted maxima at $\alpha = \pi/4 + n * \pi/2$. The maxima are found to be at $69° + n * 90°$. The result therefore corresponds to the prediction from the Jones calculus.
Since the electric fieldl signal is maximal at the angle of 69°, we use this analyzer angle for the long-term static field measurements.

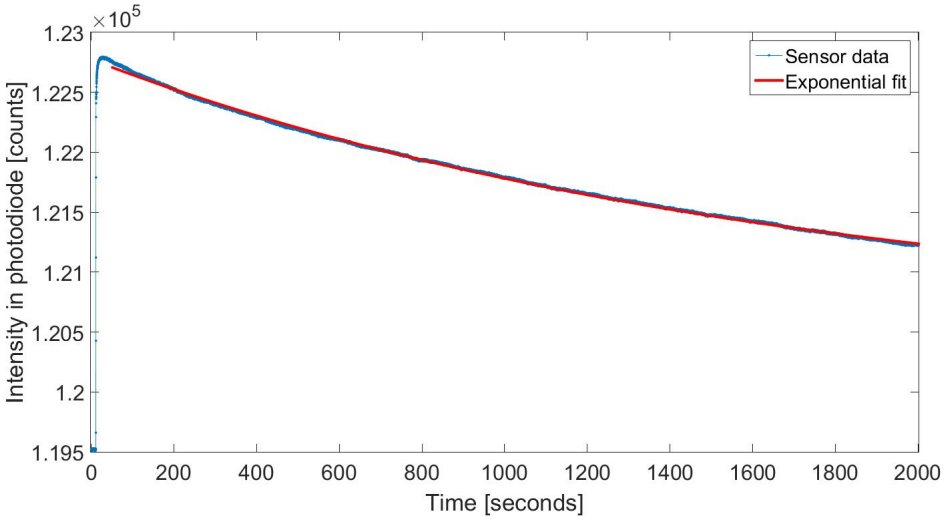

Figure 10: The intensity in the photodiode for a static electric field of 1kV/cm over a timespan of 2000 seconds. The electric field is applied shortly after t=0. Every 0.1 seconds the intensity in the photodiode is measured, which is indicated by the blue line. The red line is an exponential approximation of the data after the field is applied. The approximation closely follows the sensor signal, and deviates by less than a few % from the sensor data over these 2000 seconds.

4.4 Long-term field measurements

In this section the efficiency of the crystal for long-term static field measurements is analyzed. As explained in section 4.2.2, the space charge effect counteracts the external field with an internal field. To measure a static electric field for a longer time one needs to know the time evolution of the internal field, which is given by the charge relaxation time constant τ. When τ is known, the applied electric field can be deduced with a model for the exponential decay. An example of this is shown in figure 4.4. The sensor signal closely follows the exponential fit, so when the constant τ is known a constant electric field can be measured on this timescale. Difficulty in measuring the electric field occurs on timescales of 10^4 seconds. After this time, the internal electric field decayed back towards $E = 0$ and cannot be distinguished anymore. For an accurate long-term measurement of a static field a high value of τ is required because this allows for a slower decay of the internal electric field. The external space charge effect is caused by free charge carriers in the crystal, so minimizing the amount of free charge carriers and therefore the conductivity will increase the relaxation time of the crystal and make measurements for longer timescales possible. The conductivity of the crystal is caused by both thermal excitation of charge carriers and excitation of charge carriers by photons. Therefore the space charge

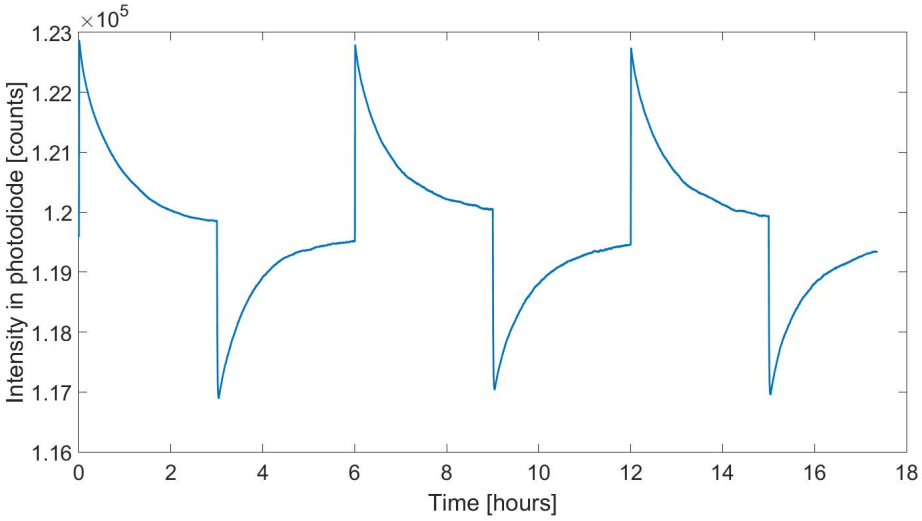

Figure 11: Long-term measurement of a static electric field. The upward jumps in intensity are caused by the application of the static field, and the downward jumps are caused by the removal of the field. The count decays exponentially towards the value for E=0 with decay rate τ

effect can be decreased by decreasing the temperature and intensity of the light. Because impurities and defects in the crystal also increase the conductivity, a crystal of high quality is required for an accurate long-term measurement.
In the following section, measurements of the relaxation time will be described for different light intensities in order to potentially increase the charge relaxation time constant for a better long-term field measurement.

4.4.1 Measuring the charge relaxation time constant

The relaxation time of the crystal is measured by applying a static electric field. The field causes the count rate to jump to a different value and over time the count rate returns to the zero-field value. The count rate decreases exponentially, since the sensor signal is approximately linear dependent on the field and the internal field exponentially decays to the zero-field value. Since the relaxation time is usually between ten minutes and an hour, the count rate with the applied static field is measured over a time of three hours. After this time, the internal field almost fully counteracts the external field, and the sensor value is close to the value without an applied electric field. After these three hours, the system is programmed to set the electric field back to zero. Since the arrangement of charges in the crystal still is still the same, there is now an internal field in the opposite direction of the external field that was present. The sensor jumps in the opposite direction and slowly decays towards the zero field value.

The decay rate of the internal field is the same as the decay rate of the external field. After three hours, the internal field approximately decayed to the zero value and the electric field can be turned back on for a second measurement. To make an accurate measurement of the charge relaxation time of the crystal, this process is repeated several times. A 1 kV/cm voltage is used to generate the static field for this measurement. An example of a measurement made with this method is shown in figure 11. It should be noted that, as can be seen in the figure, the field has not entirely returned to the zero value after the three hours of measuring. There is still a small internal field.

4.4.2 Effect of the intensity on the relaxation constant

The intensity of the light that passes through the crystal can be controlled by adjusting the aperture in front of the crystal and/or reducing the intensity of the LED. Long-term measurements have been made for three different intensities and the charge relaxation time constant τ has been measured for these intensities. In table 1 and figure 12 the results of this measurement can be seen. The intensity is expressed as a percentage of the maximum intensity. Each of the data points in this table is the result of a measurement of 12 hours or longer, so it is an average over 4 or more field jumps.

Relative intensity	τ(seconds)
100%	2289 ± 112
41%	2666 ± 84
17%	2722 ± 109

Table 1: Charge relaxation constant τ as a function of LED intensity

The data show that lowering the intensity increases the charge relaxation time constant. It can be concluded from this dependence that a relevant portion of the free charge carriers in the crystal comes from photon excitation. For a good long-term measurement, a low intensity beam is optimal. The linear approximation in figure 12 suggests that that the light is not the only source of free charge carriers, because the crystal still exhibits the space charge effect for a relative intensity of zero. There are free charge carriers provided by thermal excitation or crystal impurities.

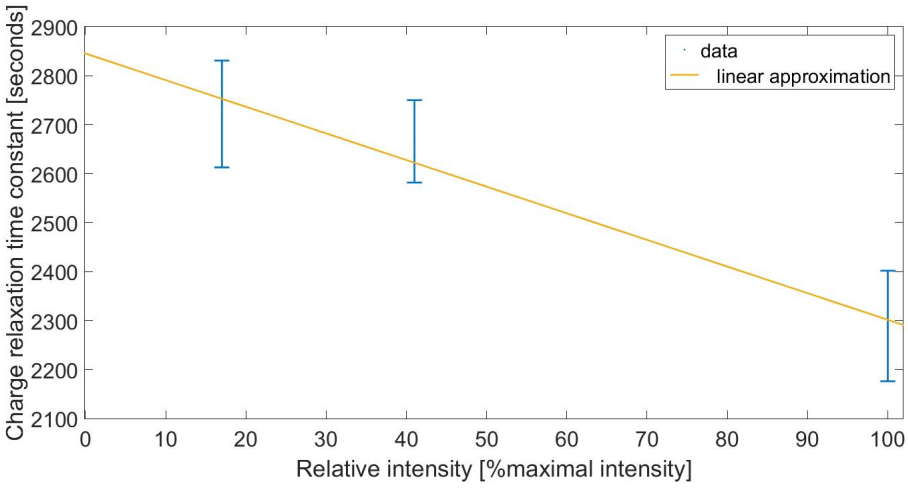

Figure 12: The charge relaxation time constant τ as a function of energy, with linear approximation

5 Conclusions

The developed Lithium Niobate electro-optic sensor can measure a static electric field for timescales of $10^3 - 10^4$ seconds. The decay of the internal field makes it impossible to measure the static field for higher timescales.
By lowering the intensity of the beam a charge relaxation time constant of (2722 ± 345) seconds could be reached. This is sufficient for measuring a static field in the EDM experiment in Juelich.
The Lithium Niobate sensor is able to measure static electric fields over a longer time than any other electro-optic field sensor. Commercially available devices can measure electric fields for a second or less, and the developed sensor is efficient for timescales that are more than three orders of magnitudes higher.

References

[1] B.Yip. *Analysis of Electric Dipole Moment Experiments and their Future Prospects*. Bachelor thesis, University of Groningen. 2015.

[2] K.Takizzwa & L.Jin. *Electro-Optic Modulation Analysis of a Y-cut Z-Propagation $LiNbO_3$ Light Modulator: Comparison with an X-Cut Z-Propagation $LiNbO_3$ Light Modulator and a Dual $LiNbO_3$ Crystal Type Modulator*. Optical Review 18, no. 2 (2011): 203-211.

[3] K.Jungmann & E.A. Dijck & J.O. Grasdijk & T.Meijknecht & A.Mohanty & N.Valappol & B.Yip & L.Willmann. *Precision Tests of Discrete Symmetries*

at Low Energies. Submitted to proceeding of Low Energy Antiproton Physics (LEAP) conference, 2016.

[4] M.Bordovski. *Electro-optic Electric Field Sensor for DC and Extra-Low-frequency Measurement*. Ph.D. Thesis, Brunel University School of Engineering and Design, 1998.

[5] Bahaa E. A. Saleh & Malvin Carl Teich. *Fundamentals of Photonics*. John Wiley & Sons. New York, 2007.

[6] A.Yariv & P. Yeh. *Optical waves in crystals, Propagation and Control of Laser radiation*. John Wiley& Sons, New York, 1984.

[7] Eugene Hecht & Alfred Zajac. *Optics*. Addison-Wesley, Reading, 1974.